Network structure enabling re-use and near full property retention in CNT sheets recycled from thermoset composites

Anastasiia Mikhalchan[1]*, *Sergio Ramos Lozano*[1], *Andrea Fernández Gorgojo*[1,2], *Carlos González*[1] *and Juan J. Vilatela*[1]*

[1] IMDEA Materials Institute, Eric Kandel 2, 28906 Getafe, Madrid, Spain
[2] Mechanical Engineering Department, Universidad Politécnica de Madrid, 28006 Madrid, Spain

* Corresponding authors. IMDEA Materials Institute, 28906 Getafe, Madrid, Spain
E-mail addresses:
anastasiia.mikhalchan@imdea.org (A. Mikhalchan),
juanjose.vilatela@imdea.org (J. J. Vilatela)

KEYWORDS: carbon nanotube sheet, recycling, structural composites, fracture toughness, conductivity

ABSTRACT

Carbon nanotubes are presently used in batteries, structural composites, and electrical conductors, at a scale of the kilotonnes/year. Their use could increase above megatonnes/year as they become available as co-products of turquoise hydrogen and displace CO_2-intensive metals. In this work we study the recycling potential of sheets of CNTs, the macroscopic architecture for battery current collectors and for structural laminate composites. We use CNT sheets produced both in our laboratory and commercially to manufacture composites with aerospace-grade epoxy resin through compression moulding. After removal of the polymer phase through pyrolysis, the sheets fully retain their structure and can be re-processed without further treatment. No introduction of chemical or orientational defects is observed. Commercial CNT sheets with areal density of 12-14 g/m^2 retain 95% of their longitudinal strength and 100% modulus and electrical conductivity. Laboratory-grade sheets with higher alignment retain over 50% of their strength (54-59%). This level of property retention enables re-use for the same application, the highest level of recycling potential, which is currently unachievable for carbon fibres recycled in short discontinuous form. It stems from the inherent toughness of the CNT network structure. As a measure of damage tolerance, we evaluate the essential work of fracture of CNT sheets (3.96 kJ/m^2 and 69 kJ/m^2 for commercial and laboratory-grade, respectively) which is in the range of tough polymers and metals.

1. INTRODUCTION

Present carbon nanotube (CNT) annual production is already in the thousands of tonnes per year. Their demand as conductive additives in batteries alone will increase above 50 kt/y by the end of this decade [1]. But annual capacity may increase to the megatonne scale if CNTs are industrially produced as co-products in the generation of turquoise hydrogen and used to displace widespread CO_2-intensive materials, such as steel, aluminium and concrete [2]. Indeed, macroscopic fibres and sheets of CNTs produced in laboratories and industry around the world have tensile mechanical properties, electrical and thermal conductivity above these materials. Reported specific tensile strength of aligned CNT fibres is regularly above 3 GPa/SG and modulus above 100 GPa/SG [3–7], equal or superior to carbon fibre. Longidutinal thermal conductivity is up to 770 W/mK [6,8] and electrical conductivity is in the order of 10^5 - 10^6 S/m [6,7,9], or as high as 10.68 MS/m, approaching copper on a mass basis after introducing of dopants [10]. Given the widespread use of CNTs today and the prospect for order-of-magnitude increases in their abundance, it is timely to start studying methods to recycle them. To the best of our knowledge, there has not been any attempt to exploit the recycling of CNT macroscale materials from their composites.

Here we focus on macroscopic sheets of CNTs infiltrated with a polymer, produced both in our laboratory and at commercial industrial facilities. Unlike dispersed CNTs, the sheets have well-defined macroscopic shape and properties [11] that, thus, facilitate evaluation of recycling potential. In addition, CNT sheets have an amenable format for large-scale application of CNTs as an engineering material. CNT sheets are effective planar conductors for use as current collector in batteries [12,13], for electromagnetic interference shielding [14] and as resistive elements [15], amongst some applications demonstrated at prototype level. CNT sheets are analogous to a non-woven fabric, the common format for reinforcing fibres in structural composites. Indeed, structural composites of CNT sheets and polymer matrixes have been widely studied [16], and increasingly in industrially-relevant formats, such as coupons, laminates or components with aligned CNTs manufactured using industrial methods [17–19].

Conventional fibre reinforced polymer composites are notoriously difficult to recycle because of the challenge to recover the fibres after removal of the polymer phase. The carbon (CF) or glass (GF) fibres easily fracture due to the introduction of defects and elimination of sizing upon removal of the polymer during recycling [20]. They are, thus, recovered at best as unsized short discontinuous fibres [21]. The CF are mainly recycled through polymer pyrolysis process, which is considered as the most developed method, despite the energy requirement for decomposing the polymer matrix. The process of CFRP recycling using renewable energy supply would result in the lowest embodied energy of 3 MJ/kg [22]. Recycled in pyrolysis individual CF filaments can

retain up to 98% of the original fibre properties, but with significantly reduced length (typically, in the range from hundreds of microns to few cm) and, thus, the macroscopic format of a particulate powder. Hence, the industrial recycling processing capacity is at the range of 10% only (about 10 kt/year [23]) and the recycled milled or chopped CF are mainly used as fillers. Using solvent-dispersion methods short recycled CF can be re-processed into non-woven mats, but with only around 6.5% of the strength and modulus of the original fibre [24], therefore, suitable for the applications in low-grade non-structural components. Higher property retention may be achieved through alignment and arranging of individual chopped filaments into the close-packed preforms, but requiring additional multi-step processing. Reports show recycled CF with low misalignment of $\pm 3^{o}$ for 65-67% of CF preform achieved by the so-called HiPerDiF process [25]; $\pm 10^{o}$ for 90% of CF preform made by using a U-channel and manual formation of tapes [26]; $\pm 10\text{-}15^{o}$ for 70% to 94% of CF preform aligned by using centrifugal forces [27,28]. Yet, these processes have a high inherent complexity and achieve fibre alignment still far below that of the virgin CF preforms ($0.9\text{-}1.3^{o}$ [29]).

A growing body of work shows that the manufacture, structure and properties of CNT fibres and sheets [30–34] is more similar to that of high-performance ductile polymers rather than brittle CF, despite similarities in chemical composition. Indeed, CNTs are envisioned as ¨the ultimate polymer¨ with highly conjugated molecules of large persistent length [35]. The yarn-like CNT fibres show a smooth yielding and plastic deformation in tension [36], with the possibility to undergo strain hardening under loading cycles [32], and a level of creep [37], similar to polymer fibres [38]. The demonstrated knot efficiency [36,39] and strength at ballistic speeds are on pair with high-performance polymers, such as Dyneema [32,34], which however, is recycled very differently, not preserving their fibrous form *per se*. On another hand, composed entirely of sp^2-hydridized carbons, CNT materials do not degrade under ambient conditions, including exposure to UV radiation, do not have the melting point or glass-transition temperature, and withstand substantial heating in air, similarly to CF [40]. The prospect is that CNT sheets and related nanostructured networks may recycle very differently from conventional monolithic fibre materials.

Here we demonstrate the possibility of recycling the macroscopic CNT sheets from thermoset composite laminates and their ability to retain their macroscopic sheet shape and their original electrical and mechanical properties. Their damage tolerance and resulting property retention upon recycling is compared to materials across different families: with conventional CF, which have a common chemical backbone and fabric format, and with polymers and ductile metals which have similarly high intrinsic toughness from microstructural plastic deformation mechanisms. This high level of recycling potential stems from the inherent damage-tolerance of

CNT sheets, assessed by the essential work of fracture concept. We show that carbon chemistry and nanoscale network structure are prerequisites for the unique combination of high strength and remarkable toughness of CNT sheets, enabling effective recycling and re-use for the same applications.

2. MATERIALS AND METHODS

2.1 Materials

CNT sheets: Aligned CNT sheets were produced by FCCVD at temperature 1300 ° C using toluene as a carbon source, under synthesis conditions described elsewhere [9,30]. The sheets were comprised of predominant population of few-layer CNTs, with high graphitic nature and Raman I_D/I_G of 0.15-0.2. About 3 to 4 km of CNT aerogel filament were collected during 1 h 45 min to 2 h 20 min at the winding rate of 28 m/min and wound continuously to form the sheet (non-woven fabric). The collected CNT sheets were then densified off-line with isopropanol and left to dry overnight to produce the freestanding ultrathin sheets with the areal density of 3-4 g/m^2 and thickness under 10 µm. The produced CNT sheets were used as-synthesized, preserving the same intrinsic macroscopic compaction and degree of alignment, without any additional post-treatments. Comparative analysis of the recycling ability was done with commercially produced sheets (Tortech Nano Fibers, Israel) with areal density of 12-14 g/m^2, thickness of ~30 µm, and moderate degree of CNT alignment. For composite manufacturing, HexPly 8552 high performance tough amine-cured epoxy film suitable for primary aerospace structures was used as matrix.

CNT plane demonstrator: The CNT sheet plane demonstrator was made of commercial CNT prepreg with areal density of 35 g/m^2 with an equivalent 8552 neat resin system, provided by Huntsman, USA. The sample served for the demonstration of the process on the larger-scale commercial prepreg and complex shape composite, without further characterization.

2.2 Methods

Composite manufacturing: Composite laminates of 10 × 10 cm reinforced with CNT sheets were manufactured by compression moulding. Each preform contained one layer of CNT sheet sandwiched between two layers of epoxy film (see example of the lay-up in *Supplementary Material, S1*). The laminates were first consolidated for 10 min at 65 ° C at a pressure of 7 bar, and then cured under pressure in the sealed vacuum-bag to ensure minimum porosity. The curing

cycle consisted of two steps (130 ° C followed by 180 ° C) at temperature ramp and dwelling time according to the recommendations of the epoxy supplier. The final composites contained 6-12 %wt. of CNT.

CNT sheet recycling: CNT sheets were recycled from the composite laminate samples (cut to dimensions of 4 × 10 cm) via thermal decomposition of polymer matrix in two steps: *(i)* treatment in inert atmosphere (decomposition of matrix at multi-step ramp up to 500 ° C in N_2: 4.25 °C/min to 270.00 °C; 0.25 °C/min to 350.00 °C; 4.25 °C/min to 500.00 °C; isothermal hold for 15.00 min) followed by *(ii)* oxidation (30 min at 500 ° C). The first step was performed under a constant flow of 5 L/min of N_2, and the oxidation step was done in air.

General characterization: Thermal stability of the materials was assessed by thermogravimetric analysis (Q50, TA Instruments) ramping at 10 °C/min from room temperature to 870°C in synthetic air. Tensile tests of as-produced and recycled CNT sheets were done on the DMA machine equipped with a load cell of 18 N at the strain rate of 1 mm/min with the gauge length of 10 mm. The samples were laser-cut by a 30 W power CO_2 laser to a dog-bone shape to assure the fracture occurred at the centre and not at the grips. Specific values of strength and modulus expressed in GPa/SG were calculated via normalization by specific gravity of the samples and used to compare the recycling performance of CNT sheets, to account any possible shrinkage caused by processing via pyrolysis. Scanning Electron microscopy (SEM) was carried out with FIB-FEG SEM Helios Nanolab 600i (FEI) at 5 kV and 0.69 nA. The SAXS patterns of CNT sheets were collected using SAXSpoint 5.0 laboratory beamline (Anton Paar, Austria), equipped with Primux 100 microfocus X-ray source (Cu) at R.T., the patterns were corrected for the transmittance and background using SAXSanalysis software (V 4.20). The full width at half maximum (FWHM), the Herman's orientation parameter and $\langle cos^2(\varphi_0)\rangle$ were calculated directly from the intensity of the azimuthal profiles fitted to a Pseudo Voigt 1 function, taking into account the 3D planar symmetry of the CNT sheets. Orientation parameters were calculated in the q range corresponding to the form factor of the CNTs [41]. Raman spectra were collected using Renishaw PLC spectrometer with 532 nm laser, at magnification of ×50 and laser power of 5 %. The obtained spectra were baseline corrected and normalized to the G-band intensity maximum. Two-probe electrical resistance (longitudinal and transversal) of CNT sheets cut to rectangular strips (0.5 cm width × 2.0 cm length) was measured using a digital multimeter and gold plated contacts with clips.

Essential Work of Fracture (EWF) tests: The tests were performed using the modified Kammrath und Weiss tensile stage with the load cell of 47 N, at the strain rate of 2 µm/s with the gauge length of about 15 mm. The double-notched samples of CNT sheets were cut using the laser cutting machine, thickness was measured by a digital micrometer, 8 µm and 20 µm for lab- and

commercially-produced CNT sheets, respectively. Three different ligament lengths were analysed: 3 mm, 2 mm, and 1 mm, which were much longer than the specimen thickness, ensuring that the material was always in a state of plane stress. We operated with the original cross-sectional area of the material and specific stress (GPa/SG) rather than true stress in order to avoid any potential overestimating of the calculated work for fracture, and because the transverse shrinkage deformation across the notch plane was small.

3. RESULTS AND DISCUSSION

3.1 Recycling potential of CNT sheets

In this work we use sheets of CNTs produced both commercially and at our laboratory. Macroscopically they resemble and handle like a thin fabric, with remakable flexibility in bending (Figure 1A) and tolerance to manipulation. The constituent CNTs are aligned through the thickness and moderately in the plane. They are synthesised through floating catalyst CVD, which results in CNT aspect ratios above 10000 [42]. Because of this extraordinay high aspect ratio, the CNTs form a network, with individual CNTs joining separate bundles (Figure 1A). This network structure resembles an aligned polymer film with crystalline microfibils linked by tie molecules (Figure 1B). Thus, despite being produced from individual aerogel filaments, their overlap and densification from an open aerogel state "fuse" them into a continuous material. For the commercial CNT sheets with modertate in-plane aligment, for example, transverse conductivity is as much as 57% of longitudinal conductivity (2.6×10^4 S/m *versus* 4.6×10^4 S/m). The continuous nanostructured network structure of CNT sheets contrasts with other graphitic carbon structures. The classical carbon fibres have a "monolithic" all-solid microstructure formed of fused crystallites joined internally by covalent bonds [43]. Carbon fibres have a diameter of a few μm, negligible porosity and the external surface which correlates with their outer diameter; there is no inherent linkage between individual macroscopic filaments (Figure 1C). Preforms of CF require holding filaments together by stitching, weaving, or introducing a polymer binder. The transverse electrical conductivity of a undirectional CF fabric, for example, T700SC, is nearly 3 orders of magnitude lower than its longitudinal value (10^2 *versus* 10^5 S/m) [44].

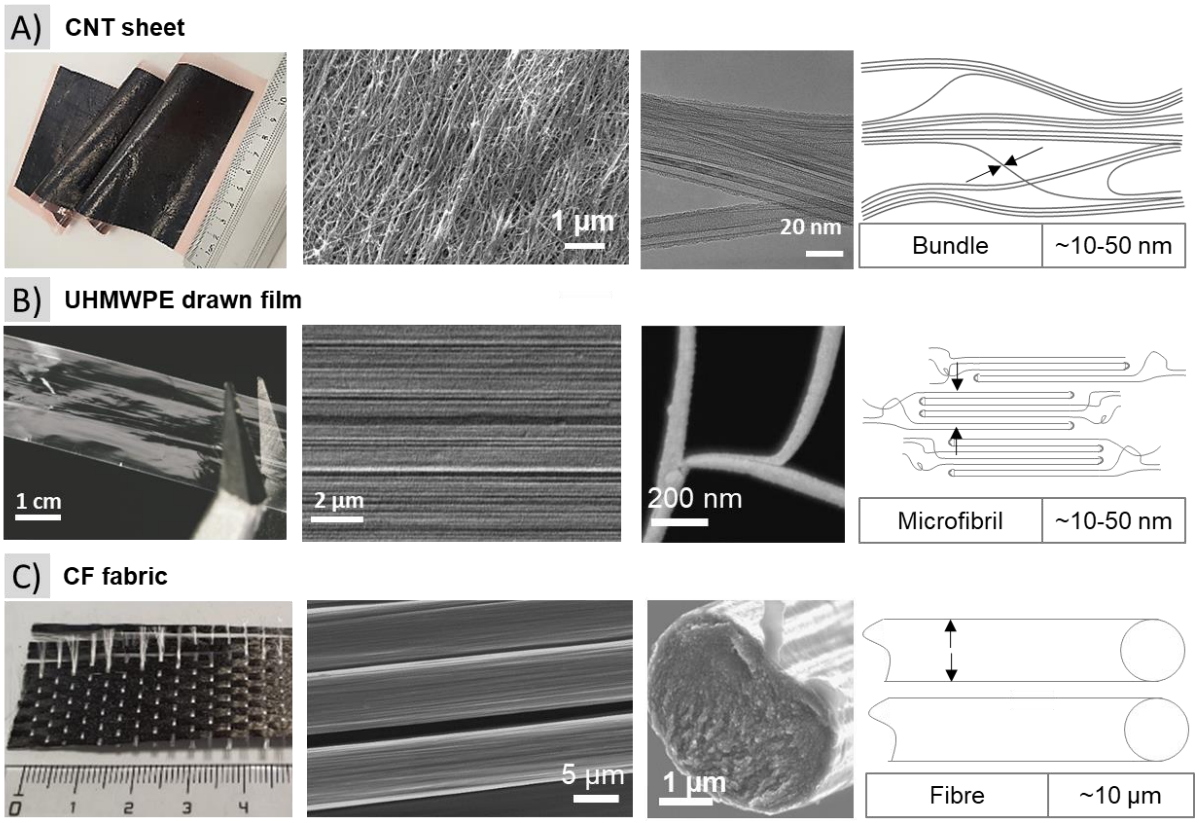

Figure 1. Overview of the materials and their structure: A) flexible CNT sheet as a continuous network of CNT bundles (reinforcing elements) with preferential alignment formed at the synthesis and collection step; B) drawn ultra-high molecular weight polyethylene (UHMWPE) film [45]; C) CF unidirectional tape. The following images are presented: macromaterial; SEM of the microstructure and individual reinforcing elements and the schematics of bundles, fibrils, and filaments. Figure B is adapted from Ref.[45] under the Creative Commons Attribution 4.0 International License.

To provide a first assessment of the potential to recycle CNT sheets, here we focus on their use in polymer composites. For this study, we used both commercial CNT sheets as well higher-grade sheets produced in our laboratory, which where infused with high-performance thermoset matrixes of the type used in aerospace and wind power structures. Figure 2A shows an example of a prepreg of CNT sheet with epoxy, which can be shaped into different articles. As an example of a complex shape with high curvature, we folded it to form a model plane (inset Figure 2A). After curing, the composite preserves its shape (Figure 2B), as expected.

To remove epoxy from the composites produced we carried out a two-stage thermal process based on a previous work on CF [46,47], adjusted here to reduce its duration and maximise resulting properties. The method consisted in a treatment in N_2 up to 500 ° C, which pyrolysed the matrix, followed by oxidation for 30 min at 500 ° C to remove the remaining char in the CNT sheet. Thermograms of the as-produced CNT sheets and their composite materials at different stages of polymer pyrolysis are included in *Supplementary Material, S2*. The CNTs exhibited high thermal stability in air at elevated temperatures, with the small mass loss (<400 ° C) related to the removing of co-synthesized non-graphitic byproducts. The samples had relatively low amount of

the residual catalyst (6.5% for IMDEA, 11.2% for commercial) and >80%wt total graphitic content (CNTs) (*Supplementary Material, Table S1*). The main degradation event related to graphitic carbon nanotubes decomposition happened at ~650-700 ⁰ C (although, small portion of CNTs decomposed at ~557 ⁰ C) for lab-produced and between 500 and 740 ⁰ C for commercially-produced CNT sheets. After polymer removal, the CNT sheet showed no visual sign of degradation. It remained as a thin, continuous sheet after recycling (Figure 2C; also *Supplementary Material, S1-D*). Its flexbility and handleability were not appreciably modified. Figures 2D shows a recycled sheet folded 7 times on itself, after which it could be unfolded back to its original shape.

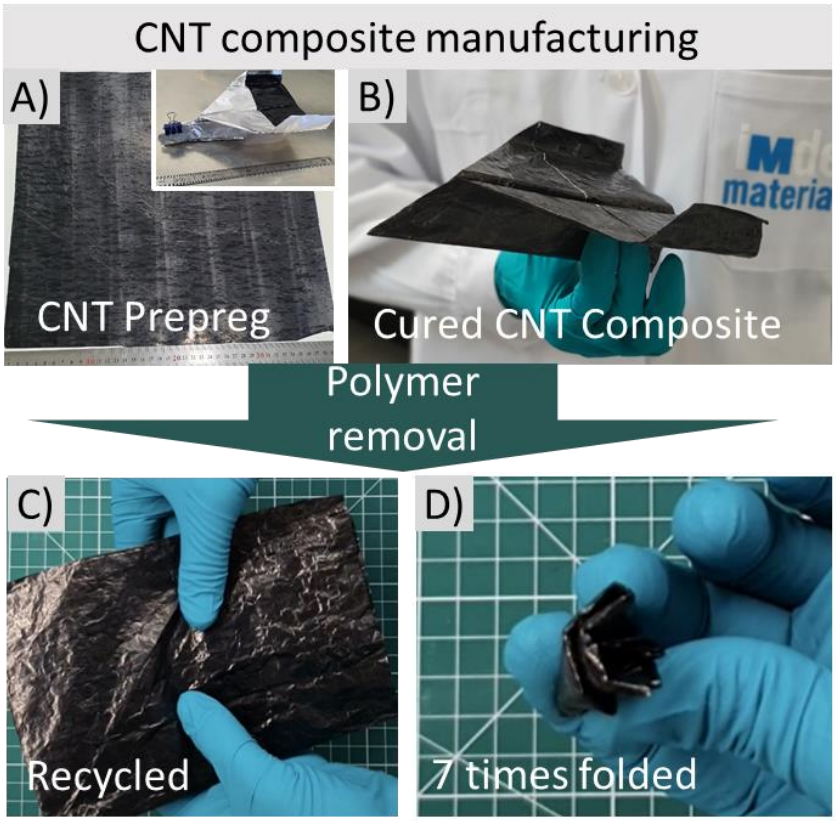

Figure 2. Demonstration of recyclability of the CNT sheet from the complex-shape composite structure: A) commercial CNT prepreg, inset: layup of the CNT plane ready for curing; B) cured CNT composite plane; C, D) flexible and robust recycled CNT sheet of ~ 17 × 22 cm size after polymer removal, which demonstrates retained ability to be handled and folded up to 7 times (See the full video of handling and folding of the recycled CNT sheet in *Supplementary Video*).

This retention of shape and handle ability in macroscopic sheets contrasts with arrays of monolithic fibres, such as CF or GF, which do not recycle as preforms but instead as discontinuous broken fibres. The comparison between the two types of materials, *i.e.*, the CNT network and conventional carbon fibres, is presented in Figure 3, which shows the retained (relative and absolute) longitudinal strength of the different materials as individual filaments and their macroscopic arrays. The ground for such comparison with CF stems from the similar chemical

structure (both CF and CNT materials are made of carbon atoms), the similar level of mechanical properties and the similar area of application in structural reinforcements. However, we highlight that the comparison of CNT sheets with CF is not direct, because the former have distinctively different nanoscale network structure formed of interconnected CNT bundles. The CF, in contrast, have orders of magnitude larger the diameter, and for instance, are more rigid, as their crystalline structure is fragile and intolerant to any substantial deformation at handling. Therefore, from the micromechanical point of view, the mechanisms of CF fracture in tension are very different from yarn-like failure in shear of CNT networks.

Due to their hierarchical interconnected nanostructure, CNT materials stand out against conventional carbon fibres, demonstrating the tensile behaviour with a clear yielding and plastic deformation where stress is transferred between oriented elements (here, CNT bundles) by shear [32,48], fracture mechanism and ductility closer to high-performance polymeric fibres [32–34], yet there are differences in potential recycling. It is known that some standard plastics such as PET [49], polyamide [50], polystyrene [51] could be recycled through dissolution from their packaging wastes. However, *high-performance* polymeric fibres are not prone to recycling in their fibre format. For example, ultra-high-molecular-weight polyethylene used in ballistic protection and high-strength ropes is recycled through deep transformation of its molecules in thermolysis into oils, waxes, and solvents~~,~~ used as raw chemicals in other common-use chemical products, such as shoe polish and mineral lubricants, but not into high-end high-strength materials of the same macroscopic fibrous form [52]. Kevlar fibres, a polymer product of a condensation reaction, are recycled mechanically into chopped down short filaments to be pulped or spun into staple yarns for reuse in non-ballistic products. So, the recycling challenges for these polymeric materials are not focused on preserving their intrinsic structure, physical form and macroscopic properties *per se*. For CNT-based macromaterials, carbon chemistry and nanoscale network structure form a basis for *the unique combination of high strength and remarkable toughness*, which is a prerequisite for effective recycling and re-use, which also serves as a ground for comparison with the engineering materials across different families (carbon, polymeric, metals), since none of them possesses a combination of mechanical and physical properties matching that of CNTs [53]. Strategically, after recycling from the polymer composite, CNT sheets could also be broken down to the "building blocks" - individualized CNTs re-dissoluble in chlorosulfonic acid offering the possibility for re-spinning the macroscopic fibres from liquid crystalline solutions of recycled CNTs, something which will be practically confirmed in the future. This possibility again drastically contrasts to conventional CF, which crystalline structure fused at high-temperature carbonization and graphitization of a polymeric precursor could not be ¨broken down¨ to individual crystallites and again re-graphitized by no means into continuous fibre filaments.

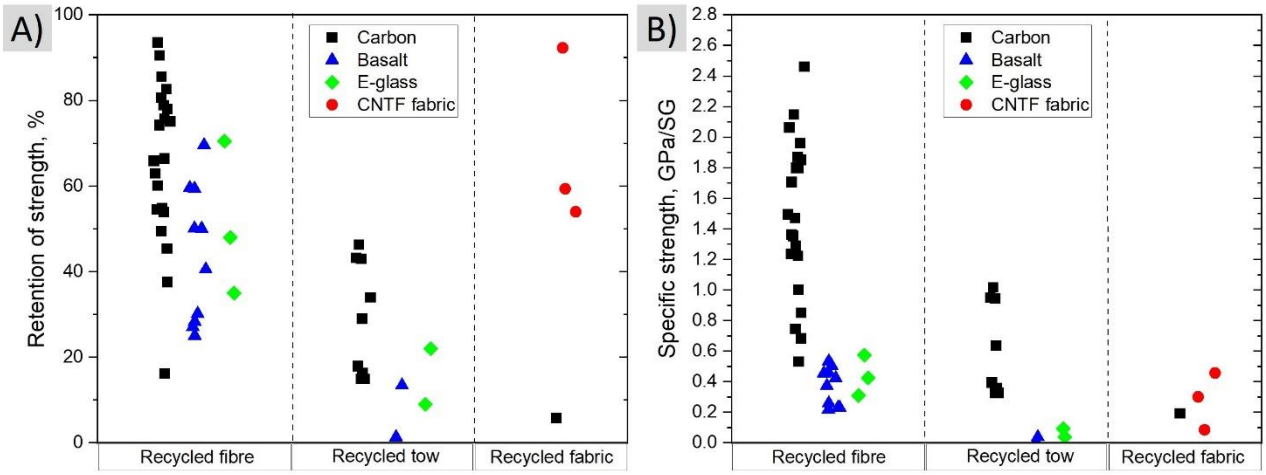

Figure 3. Comparison of strength of CNT sheets and monolithic fibre arrays after polymer removal in recycling. Tensile strength as A) a fraction of original strength and B) as specific strength for individual fibres, tows and mats/sheets of carbon [46,54–58], basalt [59–61], and E-glass [62].

In thermal recycling from thermoset composites, the commercial CNT sheets preserved 95% of their specific strength, and the higher-grade laboratory sheets over 50% (54-59%). In contrast, fabrics of monolithic fibres generally fall apart; hence reports on their properties as fabrics are very scarce. Most research works on recycled CF evaluate the retention of properties at the level of individual CF filaments, not for macroscopic arrays (tows, preforms, fabrics). In some instances, long filaments of monolithic fibres can be preserved, but their strength falls to between 95 to 16% of their original value after recycling. Individual recycled glass and basalt filaments follow the same trend, with retention of strength below 80%. For tows of recycled monolithic fibres, the drop in retained properties is also very sharp. In the only example we have found, the reported tensile strength of non-woven mat made of commercially-recycled short chopped CF is 290 MPa (0.19 GPa/SG) which is only about 5% of the strength of starting CF filaments (4-5 GPa strength and standard-intermediate modulus) [24]. The comparison in absolute units shows that laboratory grade CNT sheets are significantly above non-woven mats made of short recycled CF.

Table 1. The mechanical and electrical properties of as-produced, annealed, and recycled CNT sheets.

CNT sheets	Mechanical properties		Electrical properties	
	Specific strength, GPa/SG	**Specific modulus, GPa/SG**	**Longitudinal conductivity, S/m**	**Transversal conductivity, S/m**
IMDEA ultrathin 3-4 g/m^2				
As-produced	0.5 – 0.85	11.4 – 18.6	2.6×10^5	4.2×10^4
Recycled	0.3 – 0.46	16.2 – 28.1	2.6×10^5	–

Annealed (no polymer)	0.76	21.6	2.8×10^5	4.3×10^4
Retention after recycling (%)	54 – 59	142-151	100	–
Retention after annealing (%)	90	116	106	101
Commercial 12-14 g/m^2				
As-produced	0.093 ± 0.17	2.2 ± 0.8	4.6×10^4	2.6×10^4
Recycled	0.088 ± 0.05	8.7 ± 1.2	6.4×10^4	–
Annealed (no polymer)	0.119 ± 0.01	8.7 ± 1.1	4.9×10^4	3.4×10^4
Retention after recycling (%)	95	395	139	–
Retention after annealing (%)	128	395	106	133

The extended properties of recycled CNT sheets are summarized in Table 1. As can be seen, their electrical conductivity after recycling is identical to that of the original material in absolute terms. On the one hand, this is very relevant for re-use in energy-related applications. CNT sheets can be used as current collectors in Li-ion batteries [12,13], Zn batteries [63], and a range of other electrochemical devices [64–66], which require preserving such high level of conductivity above $\approx 10^4$ S/m. In addition, this result indicates that the conductive CNT network across the whole sheet is preserved, which implies that both the connectivity between bundles and their intrinsic conductance are largely unaltered. Indeed, we observed no introduction of either compositional or orientational defects. Electron micrographs, SAXS data and Raman spectra of the sheets before and after recycling from the thermoset composites are statistically identical (Figure 4). The calculated SAXS FWHM and Herman´s orientation parameter $\langle P_2 \rangle$ testify to the preserved alignment of CNT bundles (41° and 0.49 for as-produced versus 39° and 0.46 for recycled IMDEA ultrathin sheets; 63° and 0.38 for as-produced versus 66° and 0.36 for recycled commercial sheets). I_D/I_G band ratio of these CNT sheets, which is very sensitive to the surface concentration of oxygenated defects [67], is essentially the same (0.14 ± 0.02 for as-made, 0.11 ± 0.02 for recycled).

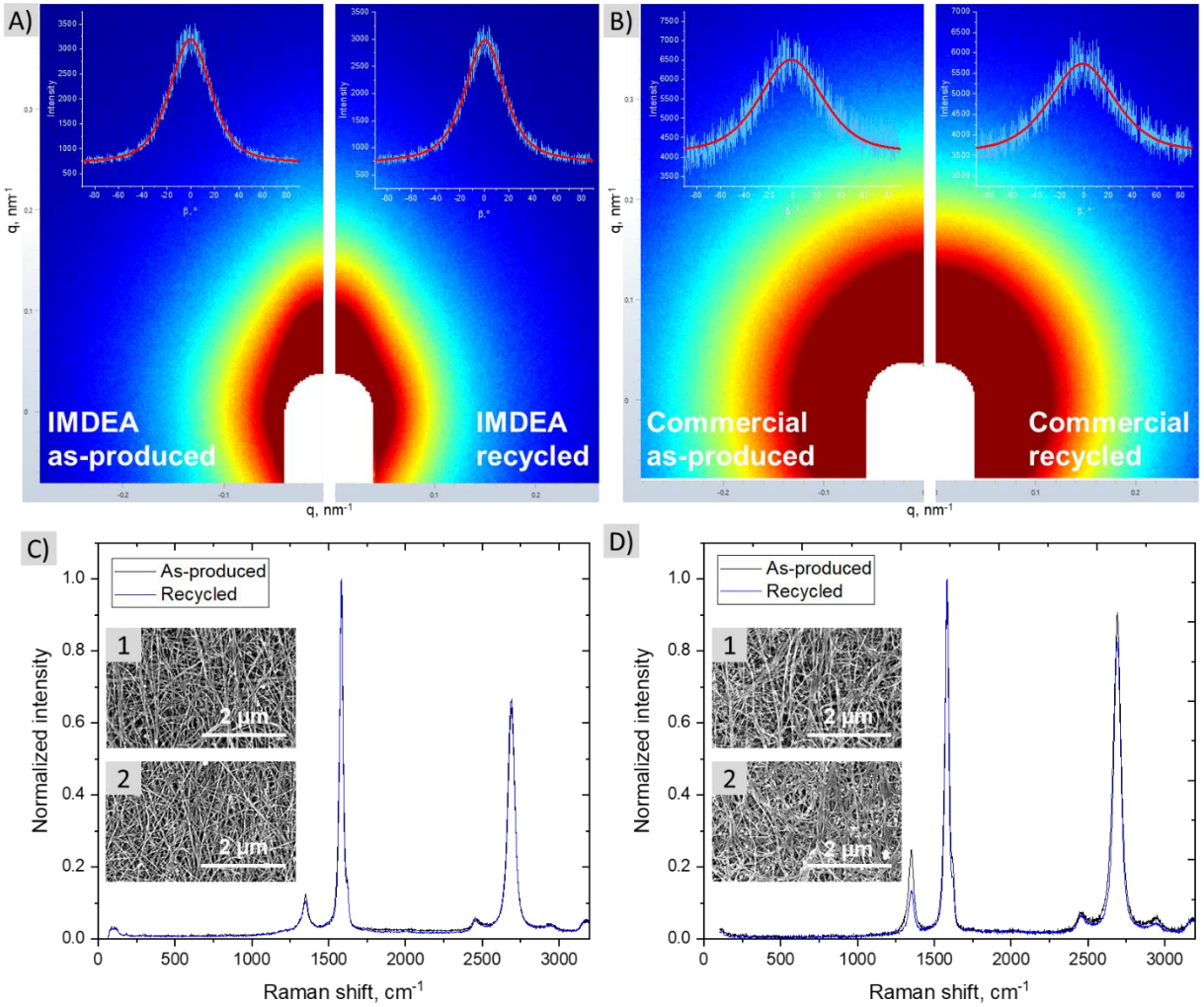

Figure 4. Structural and orientational comparison of CNT sheets before and after recycling, for both sheets produced at IMDEA and commercialy elsewhere. A), B) SAXS patterns with azimuthal profile. C),D) Raman spectra and SEM micrographs (SEM images labeled with 1 correspond to as-produced sheets, and with 2 – to recycled ones).

Mechanical tests on recycled CNT sheets showed that the tensile modulus in fact increases above its original value. This is a known effect of annealing of polymer-free CNT fibres/sheets, which we confirmed through control experiments by annealing CNT sheets without any polymer, also included in the table. Heat treating of CNT network in this temperature range (up to 500 ⁰ C) is thought to partially carbonise the residual amorphous carbonaceouse coating on the surface of CNT bundles, thus improving stress transfer between adjascent bundles through shear stress transfer at the interface [68]. It also stems from the table that the laboratory grade sheets have very high property retention at annealing, but a lower strength retention than commercial CNT sheets when recycled from the polymer composites (*Supplementary Material, S3*). We consider this retention value a *lower* estimate, and attribute it primarily to current practical limitations in handling the material during composite manufacture. The thin laboratory grade CNT sheets have an areal density of close to 4 g/m^2, which is 3.5 times below the commercial sheets. Our composite

manufacturing route is based on the industrial epoxy film and compression method designed for much thicker plies. The ultrathin CNT sheets can be damaged, for example, after the consolidation step when the protective layer is manually removed from the epoxy film, or at the following step of pressure infusion and curing, by imprinting the teflon substrate pattern, thus, generating macroscopic wrinkles (*Supplementary Material, S4*). At the same time, annealed CNT sheets, treated at the same conditions in their dry state, without polymer matrix (therefore, avoided handling in the composite manufacturing step), have shown 90% strength retention, evidence of a higher recycling potential for aligned CNT sheets.

3.2 Damage-tolerance and recycling

A conventional unidirectional fabric of continuous monolithic fibres can be considered a parallel array of filaments with individual strength following a Weibull distribution. The strength of the array results from integrating over the number of filaments. Processing during recycling decreases their Weibull modulus, for example, from 8.0 to 4.4 for TENAX E HTA40 6K CF [69], or from 5.6 to 4.3 in longer oxidation step of T300/3K CF, which reduced the tensile strength of individual filaments from 3.2 to 2.3 GPa [46,69]. This decrease in Weibull modulus indicates that the recycled fibres have a higher degree of variability in the tensile strength due to removal of sizing at pyrolysis step and introduction of surface defects, such as surface flaws. The Griffith dependence of strength on the critical flaw size is applicable for perfectly elastic and brittle CF, where the brittle failure initiates at the very small defects in the regions with misoriented crystallites [70]. It is known that the uniform thin polymeric film of sizing agent on the fibre surface can absorb some stress, reducing the presence of critical flaws and changing the crack propagation paths [71]. Removing of sizing results in greater frictional forces between fibres in arrays, which are believed to create fine-scale damage or cause growing of existing surface defects, which altogether reduce the strength. For example, in basalt fibres subjected to heat treatments at temperatures and conditions close to those used in recycling, failure initiation have always occurred from an existing surface flaw due to its growth from initial 45 nm to 300-750 nm [59]. The nominal critical defect size (the size of the critical flaw at which the fracture initiates) in virgin standard modulus T300 and AS4 fibres is 31-49 nm [72], in virgin high-performance CF, such as T800SC, T1000G, IM7, IM10 is in the order of 18-23 nm, much smaller than in basalt fibres. Therefore, monolithic fibres are commonly recovered as fluffy, non-aligned and short discontinuous fibres, which mechanical properties heavily depend on the recycling process conditions and the gauge length used for the tests [21,73]. Indeed, a look at the literature data shows a linear dependence on strength and modulus (*Supplementary Material, S5a*), indicating

that a drop in strength upon recycling is due to CF filaments in the sample not contributing to load bearing, either because they are shorter than the gauge length or because of their high misalignment.

In contrast, CNT sheets show no drop in modulus upon recycling, even when there is a decrease in tensile strength (*Supplementary Material, S5b*). We previously demonstrated that the bulk modulus of aligned CNT fibres [32] or sheets [30] can be related to the degree of alignment and shear modulus (g) of the CNTs through the Uniform Stress Transfer model (USM):

$$\frac{1}{E} = \frac{1}{e_c} + \frac{\langle cos^2(\varphi_0)\rangle}{g} \quad (1),$$

where e_c is the modulus of a CNT and $\langle cos^2(\varphi_0)\rangle$ is an orientation parameter calculated from the azimuthal intensity distribution obtained from 2D X-ray scattering or SEM imaging. USM reduces the complex macroscopic material to a network of fibrils which can deform elastically by stretching and shear, thus, it is possible to relate the modulus to the second moment of the orientation distribution function (ODF) and compare the different CNT network ensembles. Our SAXS measurements performed at 10 points across the width of a CNT sheet show no appreciable change in in-plane orientation upon recycling (*Supplementary Material, S6*). The slight increase in modulus is due to annealing increasing the shear modulus, as observed in other CNT systems [39].

We attribute the decrease in tensile strength of CNT sheets to small point defects exogenously introduced during handling, rather their potential degradation at elevated temperatures. Due to higher alignment and packing densities, and numerous inter-tube contacts, CNT ensembles are efficient hear conductors [74]. CNT sheets produced commercially and in the lab exhibit high thermal conductivity above 100 W/m·K [75], and when introduced in epoxy composites, demonstrate the thermal conductivity of 23 W/m·K or as high as 51.6 W/m·K at 10%wt and 30%vol fractions, respectively, versus 5.2 W/m·K for the composite reinforced with 30%wt T300 CF [75,76]. It is expected that CNT network would sufficiently transfer heat across the composite sample to facilitate the elimination of the polymer throughout the infiltrated network. Neither Raman nor SAXS and SEM observation of recycled samples show differences in sheets after recycling (Figure 4), thus shedding no light on the nature of the defects. They are likely to be highly localized separation of bundles, which would be undetected by either technique.

Irrespective of the still somewhat uncertain nature of defects in CNT sheets, they sustain the polymer removal process because of their high overall toughness. Whether as sheets or more aligned fibres, CNT nanotextiles are known to be tough against cutting [36] and withstand large flexural deformations, enabling knotting [36], knitting [77] and weaving [33]. Conventional reinforcing fibres, such as carbon and glass, have a linear elastic behaviour, and thus, their damage

tolerance is measured through the fracture toughness of individual filaments. CNT sheets have, instead, an elasto-plastic tensile behaviour. Their overall toughness has been previously quantified in terms of their tensile work of fracture, when simply calculated by integration of the stress-strain curve up to the break. It ranges between 10-30 J/g for sheets to 50-100 J/g for aligned CNT fibres [78], which is above the work of fracture of many individual CFs, usually under 20 J/g.

For ductile materials such as metals and polymers, which exhibit significant plastic deformations at fracture so the cracks do not grow catastrophically, the Essential Work of Fracture (EWF) concept is mostly used to characterize toughness. This more accurate description of damage tolerance separates the total work of fracture (W_f) into an essential component (w_e), related to its intrinsic toughness, and a non-essential component (w_p) that is geometry-dependent, associated with irreversible plastic deformation in the outer fracture zone:

$$W_f = W_e + W_p \qquad (2)$$

The first component is related to the materials´ resistance to crack initiation, and the second is a measure of the resistance to crack propagation. The two components are determined through mechanical tests on pre-notched specimens with different ligament length (L), assuming that the fracture process zone and the plastic deformation zone are within the ligament. The work in Equation (2) is then expressed in terms of the thickness of the specimen t and the ligament length, L:

$$W_f = w_e \cdot Lt + \beta w_p \cdot L^2 t \qquad (3)$$

Upon rearrangement, one can normalize by the specimen cross-section:

$$w_f = w_e + \beta w_p L \qquad (4)$$

where w_f is the specific work of fracture, w_e is the essential work of fracture and w_p the non-essential work of fracture, and β is a factor related to the shape of the outer plastic dissipation zone [79].

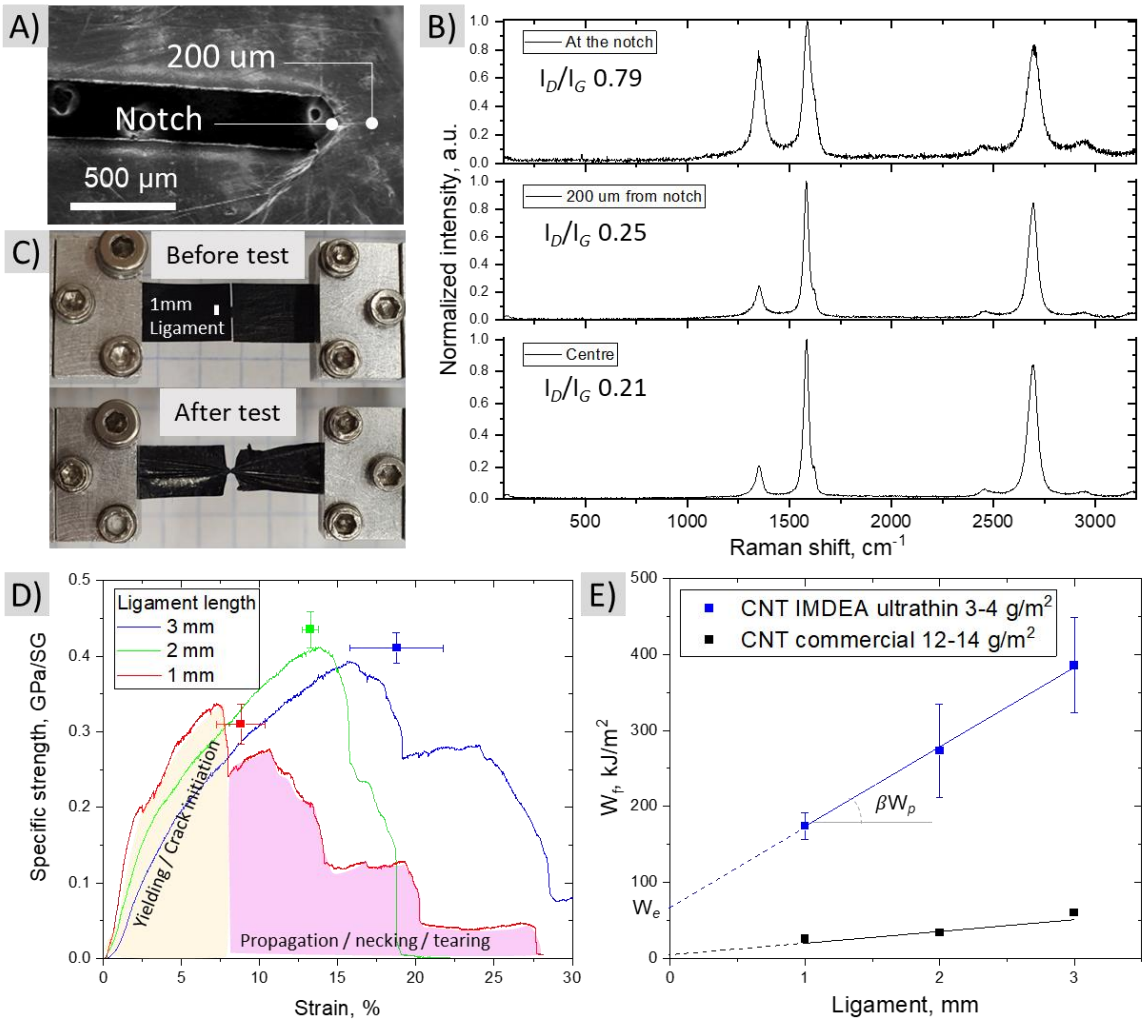

Figure 5. A) SEM of the laser-cut notch in CNT sheets; B) Raman spectra taken in several points from the notch tip; C) Photo of the DENT sample with 1 mm ligament length before and after test; D) the stress-strain curves recorded for three different ligament lengths (1 mm, 2 mm, and 3 mm) for IMDEA CNT sheets; and E) the specific total work of fracture (w_f) plotted against ligament length for CNT sheets.

Double-notched CNT sheets with different ligament length were produced by laser-cutting (Figure 5). The cutting parameters were optimized to minimize alteration of the remaining material. Using Raman spectroscopy, we could confirm that the laser effects are constrained to <200 µm of the cutting edge (the highest rise in I_D/I_G of 0.79 was measured at 2 µm distance from the notch edge), which is much smaller than the length of the smallest ligament produced of 1mm (Figure 5A, B). The EWF tests were performed on specimens with ligament lengths of 1 mm, 2 mm, and 3 mm. An example of a specimen before and after the test is presented in Figure 5C.

The self-similar stress-strain curves in Figure 5D for different ligament lengths and the observation of the material yielding without stress hardening validate the EWF model used. Closer inspection of the fracture surface shows that the material failed through predominantly lateral displacement of the crack (see *Supplementary Material, S7*). Furthermore, it is confirmed that failure occurs through damage propagation as a transversal band, i.e., that the inner fracture

process zone (IFPZ) is proportional to the ligament length and sample thickness. The outer process dissipation zone (OPDZ) is expected to extend beyond the ligament line as a volume of surrounding region of the crack.

Stress-strain curves for IMDEA-produced CNT sheets with different ligament length are included in Figure 5D (see the example of the fracture and tensile curves of commercial sheets in *Supplementary Material, S8*). They are self-similar, and have shapes commonly observed in ductile polymers and metals. The initial part represents the work from full ligament yielding and the crack initiation up to the point of highest stress. This is followed by work from propagation, including the stress redistribution in the plastic zone by plastic extending the CNT bundle network and its necking and tearing. The specific total work of fracture for different ligament lengths is shown in Figure 5E. From their linear dependence, two work of fracture components are determined by a linear regression according to Equation 4 (see *Supplementary Material, S9*).

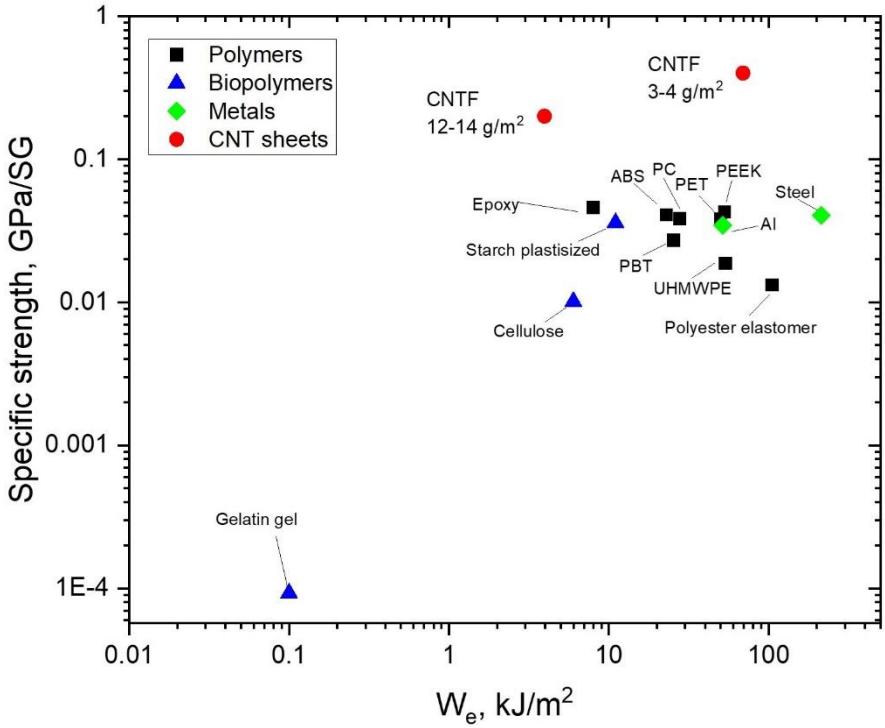

Figure 6. Comparison of the specific strength and essential work of fracture for different types of materials, including metals [80,81], polymers [82–89], and CNT sheets.

The essential work of fracture comes out as 3.96 kJ/m^2 and 69 kJ/m^2 for the commercial and laboratory-grade CNT sheets, respectively. To put these values in context, we compare them against other ductile materials, including tough metals (Al 51.5 kJ/m^2 [80], steel 213 kJ/m^2 [81]) and a range of polymers (Figure 6). We also compare their strength, normalized by specific gravity to enable comparison on an equal mass basis. The data show that CNT sheets occupy a space of both high strength and high essential work of fracture. The notable difference between laboratory-grade and commercial CNT sheets is an interesting observation, even though the essential work of

fracture concept takes into account their difference in thickness. Following the Uniform Stress Transfer model (*Eq.1* above), and plotting the compliance (E^{-1}) and the orientation parameter $\langle cos^2(\varphi_0)\rangle$ (*Supplementary Material, S10*), which we can extract from SAXS measurements, with the data for aligned CNT ensembles gathered in our previous works, we conclude that the bulk properties of CNT sheets are highly dominated by their bundle alignment. Specifically, the lab-produced CNT sheet fits the trend, and highlights the overall improvement in the CNT synthesis and collection step done by our group since the last year [30], because the as-produced sheets demonstrate higher alignment ($\langle cos^2(\varphi_0)\rangle$ of 0.117 versus 0.157). However, the commercially-produced CNT sheet with the orientation parameter of $\langle cos^2(\varphi_0)\rangle$ of 0.170 and very low modulus falls far off the trend, which we have noticed before for thick CNT tows and misaligned systems. The "orientation effect" is a well-known reason for increase w_e in polymeric materials, through increasing order of the crystalline structure or the tie molecule density, transferring stress from "weak" amorphous to "strong" crystalline phase [79]. Therefore, it can be the CNT alignment and more efficient stress transfer between aligned bundles that results in much higher essential work of fracture observed for lab-produced CNT sheets. Since the essential work of fracture depends strongly on the initial structure of the material, increased CNT network density could also lead to increase of w_e due to higher resistance to crack propagation, in analogy to the effect of molecular orientation and increased tie molecules density observed in polymers [90]. It is also noteworthy how nanostructuring increases work of fracture by orders of magnitude, compared to monolithic analogues of the same chemistry such as polycrystalline graphite (0.04 kJ/m^2) and carbon-carbon composite of CF felt (0.23 kJ/m^2) [91]. This is a mark of overall toughness for handling, and the reason the material withstands polymer removal during recycling. The encouraging prospect is that such inherent property of CNT sheets will enable recycling through other methods besides pyrolysis and from embodiment different from polymer composites.

4. CONCLUSIONS

The work explored the combination of two-step thermal treatment process and demonstrated the recycling of CNT sheets from their thermoset composites. This approach is shown on two different types of CNT sheets, including the light areal density lab-grade sheets (3-4 g/m^2) and commercial sheets (12-14 g/m^2). The recycled CNT sheets have demonstrated nearly full retention of mechanical and electrical properties after polymer matrix removal, testifying to the fact that the interconnected CNT network was preserved in its intrinsic state and without evident degradation. Good handling ability was also observed for CNT sheet recycled from the complex shape composite plane. The recycled commercial CNT sheets were re-used in the thermoset composite manufacturing for the same application, demonstrating the highest possible level of waste

hierarchy and recycling capabilities impossible for conventional monolithic fibres. The high recycling potential is ascribed to the intrinsic toughness and structural ductility of CNT sheets, which was confirmed by the Essential Work of Fracture concept. The obtained values of the w_e for CNT sheets ($3.96 – 69$ kJ/m^2) are in the range of tough polymers, combined with higher specific strength.

AUTHOR'S CONTRIBUTION STATEMENT

Anastasiia Mikhalchan: conceptualization, methodology, investigation, data processing, data curation, writing – original draft, writing – review & editing, supervision. **Sergio Ramos Lozano**: investigation, validation, data processing. **Andrea Fernández Gorgojo**: investigation, writing – review & editing. **Carlos González**: writing – review & editing, supervision. **Juan J. Vilatela**: conceptualization, writing – original draft, writing – review & editing, supervision, finding acquisition.

DECLARATION OF COMPETING INTEREST

The authors declare that they have no known competing financial interests or personal relationships that could have appeared to influence the work reported in this paper.

ACKNOWLEDGMENTS

A.M. and J.J.V. acknowledge The Carbon Hub for the financial support. The authors thank Dr Yunfu Ou and Dr Álvaro Ridruejo for discussions on the Essential Work of Fracture concept, Carlos del Castillo Montull for technical assistance with tensile tests of notched CNT sheets, José Luis Jiménez for technical assistance with hot press operation, and Dr Afshin Pendashteh for technical assistance with SAXS beamline operation. This work was supported by the European Union Horizon 2020 Programme under grant agreement 101045394 (ERC-2021-COG, UNIYARNS).

Appendix A. Supplementary data

Supplementary data to this article can be found online at http://...

REFERENCES

[1] M. Sapp, LG Chem constructing world's largest single-line carbon nanotubes manufacturing plant, Biofuels Dig. (2022). https://www.biofuelsdigest.com/bdigest/2022/08/30/lg-chem-constructing-worlds-largest-single-line-carbon-nanotubes-manufacturing-plant/.

[2] M. Pasquali, C. Mesters, Opinion: We can use carbon to decarbonize—and get hydrogen for free, Proc. Natl. Acad. Sci. 118 (2021) e2112089118. https://doi.org/10.1073/pnas.2112089118.

[3] H. Cho, H. Lee, E. Oh, S.H. Lee, J. Park, H.J. Park, S.B. Yoon, C.H. Lee, G.H. Kwak, W.J. Lee, J. Kim, J.E. Kim, K.H. Lee, Hierarchical structure of carbon nanotube fibers, and the

change of structure during densification by wet stretching, Carbon N. Y. 136 (2018) 409–416. https://doi.org/10.1016/J.CARBON.2018.04.071.

[4] E. Oh, H. Cho, J. Kim, J.E. Kim, Y. Yi, J. Choi, H. Lee, Y.H. Im, K.H. Lee, W.J. Lee, Super-Strong Carbon Nanotube Fibers Achieved by Engineering Gas Flow and Postsynthesis Treatment, ACS Appl. Mater. Interfaces. 12 (2020). https://doi.org/10.1021/acsami.9b19861.

[5] J. Lee, D.-M. Lee, Y. Jung, J. Park, H.S. Lee, Y.-K. Kim, C.R. Park, H.S. Jeong, S.M. Kim, Direct spinning and densification method for high-performance carbon nanotube fibers, Nat. Commun. 10 (2019) 2962. https://doi.org/10.1038/s41467-019-10998-0.

[6] X. Zhang, M. De Volder, W. Zhou, L. Issman, X. Wei, A. Kaniyoor, J.T. Portas, F. Smail, Z. Wang, Y. Wang, H. Liu, W. Zhou, J. Elliott, S. Xie, A. Boies, Simultaneously enhanced tenacity, rupture work, and thermal conductivity of carbon nanotube fibers by raising effective tube portion, Sci. Adv. 8 (2022). https://doi.org/10.1126/sciadv.abq3515.

[7] K. Wu, B. Wang, Y. Niu, W. Wang, C. Wu, T. Zhou, L. Chen, X. Zhan, Z. Wan, S. Wang, Z. Yang, Y. Zhang, L. Zhang, Y. Zhang, Z. Yong, M. Jian, Q. Li, Carbon nanotube fibers with excellent mechanical and electrical properties by structural realigning and densification, Nano Res. 16 (2023) 12762–12771. https://doi.org/10.1007/s12274-023-6157-1.

[8] T.S. Gspann, S.M. Juckes, J.F. Niven, M.B. Johnson, J.A. Elliott, M.A. White, A.H. Windle, High thermal conductivities of carbon nanotube films and micro-fibres and their dependence on morphology, Carbon N. Y. 114 (2017). https://doi.org/10.1016/j.carbon.2016.12.006.

[9] A. Mikhalchan, M. Vila, L. Arévalo, J.J. Vilatela, Simultaneous improvements in conversion and properties of molecularly controlled CNT fibres, Carbon N. Y. 179 (2021) 417–424. https://doi.org/10.1016/j.carbon.2021.04.033.

[10] C. Madrona, S. Hong, D. Lee, J. García-Pérez, J.M. Guevara-Vela, R.B. Gavito, A. Mikhalchan, J. Llorca, B.-C. Ku, D. Granados, J.Y. Hwang, J.J. Vilatela, Continuous intercalation compound fibers of bromine wires and aligned CNTs for high-performance conductors, Carbon N. Y. 204 (2023) 211–218. https://doi.org/https://doi.org/10.1016/j.carbon.2022.12.041.

[11] A. Mikhalchan, A. Pendashteh, J.J. Vilatela, Properties, applications and industrialization of carbon nanotube materials from hydrocarbons cracking, in: Adv. Chem. Eng., 2023. https://doi.org/10.1016/bs.ache.2023.07.001.

[12] N. Boaretto, J. Almenara, A. Mikhalchan, R. Marcilla, J.J. Vilatela, A Route to High-Toughness Battery Electrodes, ACS Appl. Energy Mater. 2 (2019).

https://doi.org/10.1021/acsaem.9b00906.

[13] N. Boaretto, B. Dávila, S. Sevilla, G. García, A. Mikhalchan, M. Rana, A. Yusuf, L. Ubierna Martinez, M. Castillo García, J. Palma, D.Y. Wang, R. Marcilla, J. José Vilatela, Thermoconformable, Flexible Lithium-Ion Batteries, Adv. Mater. Technol. 7 (2022). https://doi.org/10.1002/admt.202101635.

[14] L. Issman, M. Alper, S. Howard, C. Karch, S. Yeshurun, M. Pick, A. Boies, Direct-spun CNT textiles for high-performance electromagnetic interference shielding in an ultra-wide bandwidth, Carbon N. Y. 206 (2023) 166–180. https://doi.org/https://doi.org/10.1016/j.carbon.2023.02.013.

[15] X. Yao, S.C. Hawkins, B.G. Falzon, An advanced anti-icing/de-icing system utilizing highly aligned carbon nanotube webs, Carbon N. Y. 136 (2018) 130–138. https://doi.org/https://doi.org/10.1016/j.carbon.2018.04.039.

[16] A. Mikhalchan, J.J. Vilatela, A perspective on high-performance CNT fibres for structural composites, Carbon N. Y. 150 (2019). https://doi.org/10.1016/j.carbon.2019.04.113.

[17] J.-W. Kim, J.M. Gardner, G. Sauti, R.A. Wincheski, B.D. Jensen, K.E. Wise, E.J. Siochi, Multi-scale hierarchical carbon nanotube fiber reinforced composites towards enhancement of axial/transverse strength and fracture toughness, Compos. Part A Appl. Sci. Manuf. 167 (2023) 107449. https://doi.org/https://doi.org/10.1016/j.compositesa.2023.107449.

[18] C. Evers, B. Vondrasek, C. Jolowsky, J.G. Park, M. Czabaj, B. Ku, K. Thagard, G. Odegard, Z. Liang, Scalable high tensile modulus composite laminates using carbon nanotube yarns, 2022. https://doi.org/10.26434/chemrxiv-2022-6fcwk.

[19] J.W. Kim, G. Sauti, R.J. Cano, R.A. Wincheski, J.G. Ratcliffe, M. Czabaj, N.W. Gardner, E.J. Siochi, Assessment of carbon nanotube yarns as reinforcement for composite overwrapped pressure vessels, Compos. Part A Appl. Sci. Manuf. 84 (2016). https://doi.org/10.1016/j.compositesa.2016.02.003.

[20] D. He, V.K. Soo, F. Stojcevski, W. Lipiński, L.C. Henderson, P. Compston, M. Doolan, The effect of sizing and surface oxidation on the surface properties and tensile behaviour of recycled carbon fibre: An end-of-life perspective, Compos. Part A Appl. Sci. Manuf. 138 (2020). https://doi.org/10.1016/j.compositesa.2020.106072.

[21] S.R. Naqvi, H.M. Prabhakara, E.A. Bramer, W. Dierkes, R. Akkerman, G. Brem, A critical review on recycling of end-of-life carbon fibre/glass fibre reinforced composites waste using pyrolysis towards a circular economy, Resour. Conserv. Recycl. 136 (2018). https://doi.org/10.1016/j.resconrec.2018.04.013.

[22] K. Kooduvalli, J. Unser, S. Ozcan, U.K. Vaidya, Embodied Energy in Pyrolysis and Solvolysis Approaches to Recycling for Carbon Fiber-Epoxy Reinforced Composite Waste

Streams, Recycling. 7 (2022). https://doi.org/10.3390/recycling7010006.

[23] J. Zhang, V.S. Chevali, H. Wang, C.H. Wang, Current status of carbon fibre and carbon fibre composites recycling, Compos. Part B Eng. 193 (2020). https://doi.org/10.1016/j.compositesb.2020.108053.

[24] G-TEX M carbon fibre nonwoven mats product by GEN2 carbon, (n.d.). https://www.gen2carbon.com/product/g-tex-m/.

[25] H. Yu, K.D. Potter, M.R. Wisnom, A novel manufacturing method for aligned discontinuous fibre composites (High Performance-Discontinuous Fibre method), Compos. Part A Appl. Sci. Manuf. 65 (2014). https://doi.org/10.1016/j.compositesa.2014.06.005.

[26] G. Oliveux, J.L. Bailleul, A. Gillet, O. Mantaux, G.A. Leeke, Recovery and reuse of discontinuous carbon fibres by solvolysis: Realignment and properties of remanufactured materials, Compos. Sci. Technol. 139 (2017). https://doi.org/10.1016/j.compscitech.2016.11.001.

[27] S.J. Pickering, Z. Liu, T.A. Turner, K.H. Wong, Applications for carbon fibre recovered from composites, in: IOP Conf. Ser. Mater. Sci. Eng., 2016. https://doi.org/10.1088/1757-899X/139/1/012005.

[28] N. van de Werken, M.S. Reese, M.R. Taha, M. Tehrani, Investigating the effects of fiber surface treatment and alignment on mechanical properties of recycled carbon fiber composites, Compos. Part A Appl. Sci. Manuf. 119 (2019). https://doi.org/10.1016/j.compositesa.2019.01.012.

[29] K.K. Kratmann, M.P.F. Sutcliffe, L.T. Lilleheden, R. Pyrz, O.T. Thomsen, A novel image analysis procedure for measuring fibre misalignment in unidirectional fibre composites, Compos. Sci. Technol. 69 (2009). https://doi.org/10.1016/j.compscitech.2008.10.020.

[30] A. Mikhalchan, C. Madrona, L. Arévalo, M. Malfois, J.J. Vilatela, Improved alignment and stress transfer in CNT fibre fabrics studied by in situ X-ray and Raman during wet-drawing, Carbon N. Y. 197 (2022) 368–377. https://doi.org/10.1016/j.carbon.2022.06.045.

[31] B. Alemán, V. Reguero, B. Mas, J.J. Vilatela, Strong Carbon Nanotube Fibers by Drawing Inspiration from Polymer Fiber Spinning, ACS Nano. 0 (n.d.) null. https://doi.org/10.1021/acsnano.5b02408.

[32] J.C. Fernández-Toribio, B. Alemán, Á. Ridruejo, J.J. Vilatela, Tensile properties of carbon nanotube fibres described by the fibrillar crystallite model, Carbon N. Y. 133 (2018) 44–52. https://doi.org/10.1016/j.carbon.2018.03.006.

[33] F. Smail, A. Boies, A. Windle, Direct spinning of CNT fibres: Past, present and future scale up, Carbon N. Y. 152 (2019) 218–232. https://doi.org/10.1016/j.carbon.2019.05.024.

[34] T.S. Gspann, N.H.H. Ngern, P.J. Kiley, P.A. McKeown, J.S. Bulmer, A.H. Windle, V.B.C.

Tan, J.A. Elliott, A comparative study of the tensile failure of carbon nanotube, Dyneema and carbon fibre tows over six orders of strain rate, Carbon N. Y. 164 (2020). https://doi.org/10.1016/j.carbon.2020.03.051.

[35] M.J. Green, N. Behabtu, M. Pasquali, W.W. Adams, Nanotubes as polymers, Polymer (Guildf). 50 (2009) 4979–4997. https://doi.org/10.1016/j.polymer.2009.07.044.

[36] J.J. Vilatela, A.H. Windle, Yarn-like carbon nanotube fibers, Adv. Mater. 22 (2010). https://doi.org/10.1002/adma.201002131.

[37] J.C. Stallard, W. Tan, F.R. Smail, T.S. Gspann, A.M. Boies, N.A. Fleck, The mechanical and electrical properties of direct-spun carbon nanotube mats, Extrem. Mech. Lett. 21 (2018) 65–75. https://doi.org/10.1016/j.eml.2018.03.003.

[38] S.R. Allen, A.G. Filippov, R.J. Farris, E.L. Thomas, Macrostructure and mechanical behavior of fibers of poly- p- phenylene benzobisthiazole, J. Appl. Polym. Sci. 26 (1981). https://doi.org/10.1002/app.1981.070260127.

[39] D. Lee, S.G. Kim, S. Hong, C. Madrona, Y. Oh, M. Park, N. Komatsu, L.W. Taylor, B. Chung, J. Kim, J.Y. Hwang, J. Yu, D.S. Lee, H.S. Jeong, N.H. You, N.D. Kim, D.-Y. Kim, H.S. Lee, K.-H. Lee, J. Kono, G. Wehmeyer, M. Pasquali, J.J. Vilatela, S. Ryu, B.-C. Ku, Ultrahigh strength, modulus, and conductivity of graphitic fibers by macromolecular coalescence, Sci. Adv. 8 (2022) eabn0939. https://doi.org/10.1126/sciadv.abn0939.

[40] J.J. Vilatela, A.H. Windle, A Multifunctional yarn made of carbon nanotubes, J. Eng. Fiber. Fabr. 7 (2012). https://doi.org/10.1177/155892501200702s04.

[41] J.C. Fernández-Toribio, A. Mikhalchan, C. Santos, Á. Ridruejo, J.J. Vilatela, Understanding cooperative loading in carbon nanotube fibres through in-situ structural studies during stretching, Carbon N. Y. 156 (2020) 430–437. https://doi.org/10.1016/J.CARBON.2019.09.070.

[42] S.H. Lee, J. Park, J.H. Park, D.M. Lee, A. Lee, S.Y. Moon, S.Y. Lee, H.S. Jeong, S.M. Kim, Deep-injection floating-catalyst chemical vapor deposition to continuously synthesize carbon nanotubes with high aspect ratio and high crystallinity, Carbon N. Y. 173 (2021). https://doi.org/10.1016/j.carbon.2020.11.065.

[43] P. Morgan, Carbon Fibers and Their Composites, CRC Press, 2005.

[44] N. Athanasopoulos, V. Kostopoulos, Prediction and experimental validation of the electrical conductivity of dry carbon fiber unidirectional layers, Compos. Part B Eng. 42 (2011). https://doi.org/10.1016/j.compositesb.2011.04.008.

[45] Y. Xu, D. Kraemer, B. Song, Z. Jiang, J. Zhou, J. Loomis, J. Wang, M. Li, H. Ghasemi, X. Huang, X. Li, G. Chen, Nanostructured polymer films with metal-like thermal conductivity, Nat. Commun. 10 (2019). https://doi.org/10.1038/s41467-019-09697-7.

[46] A. Fernández, C.S. Lopes, C. González, F.A. López, Characterization of Carbon Fibers Recovered by Pyrolysis of Cured Prepregs and Their Reuse in New Composites, in: Recent Dev. F. Carbon Fibers, 2018. https://doi.org/10.5772/intechopen.74281.

[47] A. Gorgojo, C. Lopes, R. Villoria, C. González, F. López, Recovering recycled carbon fiber by pyrolysis of cured prepregs, Rev. Mater. Compuestos. (2022). https://doi.org/10.23967/r.matcomp.2018.07.003.

[48] J.J. Vilatela, J.A. Elliott, A.H. Windle, A Model for the Strength of Yarn-like Carbon Nanotube Fibers, ACS Nano. 5 (2011) 1921–1927. https://doi.org/10.1021/nn102925a.

[49] N. George, T. Kurian, Recent developments in the chemical recycling of postconsumer poly(ethylene terephthalate) Waste, Ind. Eng. Chem. Res. 53 (2014). https://doi.org/10.1021/ie501995m.

[50] V. Hirschberg, D. Rodrigue, Recycling of polyamides: Processes and conditions, J. Polym. Sci. 61 (2023). https://doi.org/10.1002/pol.20230154.

[51] M. Schlummer, A. Maurer, S. Wagner, A. Berrang, T. Fell, F. Knappich, Recycling of flame retarded waste polystyrene foams (EPS and XPS) to PS granules free of hexabromocyclododecane (HBCDD), Adv. Recycl. Waste Manag. 02 (2017). https://doi.org/10.4172/2475-7675.1000131.

[52] L. Warren, Dyneema is now recyclable, thanks to new collaboration with clean-tech company, (2021). https://sourcingjournal.com/denim/denim-innovations/dsm-dyneema-clariter-chemical-recycling-circularity-254315/.

[53] W. Lu, Q. Li, T.-W. Chou, Carbon nanotube based fibers, in: P.W.R. Beaumont, C.H. Zweben (Eds.), Compr. Compos. Mater. II, Elsevier, 2018: pp. 13–40. https://doi.org/10.1016/B978-0-12-803581-8.09875-1.

[54] A. Greco, A. Maffezzoli, G. Buccoliero, F. Caretto, G. Cornacchia, Thermal and chemical treatments of recycled carbon fibres for improved adhesion to polymeric matrix, J. Compos. Mater. 47 (2013). https://doi.org/10.1177/0021998312440133.

[55] J.S. Jeong, K.W. Kim, K.H. An, B.J. Kim, Fast recovery process of carbon fibers from waste carbon fibers-reinforced thermoset plastics, J. Environ. Manage. 247 (2019). https://doi.org/10.1016/j.jenvman.2019.07.002.

[56] K.W. Kim, H.M. Lee, J.H. An, D.C. Chung, K.H. An, B.J. Kim, Recycling and characterization of carbon fibers from carbon fiber reinforced epoxy matrix composites by a novel super-heated-steam method, J. Environ. Manage. 203 (2017). https://doi.org/10.1016/j.jenvman.2017.05.015.

[57] J. Yang, J. Liu, W. Liu, J. Wang, T. Tang, Recycling of carbon fibre reinforced epoxy resin composites under various oxygen concentrations in nitrogen-oxygen atmosphere, J. Anal.

Appl. Pyrolysis. 112 (2015). https://doi.org/10.1016/j.jaap.2015.01.017.

[58] M. Návrat, J. Závada, V. Glogarová, The Influence of Pyrolitic Degradation on Mechanical Properties of Carbon Fibres within Recycling Composite Materials, Geosci. Eng. 63 (2018). https://doi.org/10.1515/gse-2017-0017.

[59] T. Bhat, D. Fortomaris, E. Kandare, A.P. Mouritz, Properties of thermally recycled basalt fibres and basalt fibre composites, J. Mater. Sci. 53 (2018). https://doi.org/10.1007/s10853-017-1672-7.

[60] F. Sarasini, J. Tirillò, M.C. Seghini, Influence of thermal conditioning on tensile behaviour of single basalt fibres, Compos. Part B Eng. 132 (2018). https://doi.org/10.1016/j.compositesb.2017.08.014.

[61] J. Tirillo, F. Sarasini, L. Di Fausto, C. Gonzalez, A. Fernandez, C.S. Lopes, Recycled basalt fibres: fracture toughness evaluation and strength regeneration, in: ECCM18 - 18th Eur. Conf. Compos. Mater., Athens, Greece, 2018.

[62] S. Feih, E. Boiocchi, G. Mathys, Z. Mathys, A.G. Gibson, A.P. Mouritz, Mechanical properties of thermally-treated and recycled glass fibres, Compos. Part B Eng. 42 (2011). https://doi.org/10.1016/j.compositesb.2010.12.020.

[63] A. Pendashteh, J. Palma, M. Anderson, J.J. Vilatela, R. Marcilla, Doping of self-standing CNT fibers: promising flexible air-cathodes for high-energy-density structural Zn–air batteries, ACS Appl. Energy Mater. 1 (2018) 2434–2439.

[64] C. Santos, I. V. Rodríguez, J.J. Lado, M. Vila, E. García-Quismondo, M.A. Anderson, J. Palma, J.J. Vilatela, Low-energy consumption, free-form capacitive deionization through nanostructured networks, Carbon N. Y. 176 (2021). https://doi.org/10.1016/j.carbon.2021.01.148.

[65] E. Senokos, V. Reguero, L. Cabana, J. Palma, R. Marcilla, J.J. Vilatela, Large-Area, All-Solid, and Flexible Electric Double Layer Capacitors Based on CNT Fiber Electrodes and Polymer Electrolytes, Adv. Mater. Technol. 2 (2017) 1600290. https://doi.org/10.1002/admt.201600290.

[66] E. Senokos, M. Rana, M. Vila, J. Fernandez-Cestau, R.D. Costa, R. Marcilla, J.J. Vilatela, Transparent and flexible high-power supercapacitors based on carbon nanotube fibre aerogels, Nanoscale. 12 (2020). https://doi.org/10.1039/d0nr04646a.

[67] D. Iglesias, E. Senokos, B. Alemán, L. Cabana, C. Navío, R. Marcilla, M. Prato, J.J. Vilatela, S. Marchesan, Gas-Phase Functionalization of Macroscopic Carbon Nanotube Fiber Assemblies: Reaction Control, Electrochemical Properties, and Use for Flexible Supercapacitors, ACS Appl. Mater. Interfaces. 10 (2018) 5760–5770. https://doi.org/10.1021/acsami.7b15973.

[68] A.M. Beese, X. Wei, S. Sarkar, R. Ramachandramoorthy, M.R. Roenbeck, A. Moravsky, M. Ford, F. Yavari, D.T. Keane, R.O. Loutfy, S.B.T. Nguyen, H.D. Espinosa, Key factors limiting carbon nanotube yarn strength: Exploring processing-structure-property relationships, ACS Nano. 8 (2014). https://doi.org/10.1021/nn5045504.

[69] A. Fernández Gorgojo, Recovery and re-use of carbon fibres from recycled end-of-life epoxy based composites, Universidad Carlos III de Madrid, 2022.

[70] W.N. Reynolds, J. V. Sharp, Crystal shear limit to carbon fibre strength, Carbon N. Y. 12 (1974). https://doi.org/10.1016/0008-6223(74)90018-9.

[71] R.L. Zhang, Y.D. Huang, D. Su, L. Liu, Y.R. Tang, Influence of sizing molecular weight on the properties of carbon fibers and its composites, Mater. Des. 34 (2012). https://doi.org/10.1016/j.matdes.2011.05.021.

[72] X. Zhou, A. Belianinov, A.K. Naskar, Analyzing carbon fiber structures observed by helium ion microscopy and their mechanical properties, Carbon Trends. 4 (2021). https://doi.org/10.1016/j.cartre.2021.100055.

[73] G. Oliveux, L.O. Dandy, G.A. Leeke, Current status of recycling of fibre reinforced polymers: Review of technologies, reuse and resulting properties, Prog. Mater. Sci. 72 (2015). https://doi.org/10.1016/j.pmatsci.2015.01.004.

[74] L. Qiu, X. Zhang, Z. Guo, Q. Li, Interfacial heat transport in nano-carbon assemblies, Carbon N. Y. 178 (2021). https://doi.org/10.1016/j.carbon.2021.02.105.

[75] X. Zhang, W. Tan, F. Smail, M. De Volder, N. Fleck, A. Boies, High-fidelity characterization on anisotropic thermal conductivity of carbon nanotube sheets and on their effects of thermal enhancement of nanocomposites, Nanotechnology. 29 (2018). https://doi.org/10.1088/1361-6528/aacd7b.

[76] J.J. Vilatela, R. Khare, A.H. Windle, The hierarchical structure and properties of multifunctional carbon nanotube fibre composites, Carbon N. Y. 50 (2012) 1227–1234. https://doi.org/10.1016/j.carbon.2011.10.040.

[77] X. Luo, W. Weng, Y. Liang, Z. Hu, Y. Zhang, J. Yang, L. Yang, S. Yang, M. Zhu, H.M. Cheng, Multifunctional fabrics of carbon nanotube fibers, J. Mater. Chem. A. 7 (2019). https://doi.org/10.1039/c9ta01474h.

[78] A. Mikhalchan, J.J. Vilatela, A perspective on high-performance CNT fibres for structural composites, Carbon N. Y. 150 (2019) 191–215. https://doi.org/10.1016/j.carbon.2019.04.113.

[79] T. Bárány, T. Czigány, J. Karger-Kocsis, Application of the essential work of fracture (EWF) concept for polymers, related blends and composites: A review, Prog. Polym. Sci. 35 (2010). https://doi.org/10.1016/j.progpolymsci.2010.07.001.

[80] M.Y. Abdellah, Essential work of fracture assessment for thin aluminium strips using finite element analysis, Eng. Fract. Mech. 179 (2017). https://doi.org/10.1016/j.engfracmech.2017.04.042.

[81] S.K. Chandra, R. Sarkar, A.D. Bhowmick, P.S. De, P.C. Chakraborti, S.K. Ray, Fracture toughness evaluation of interstitial free steel sheet using Essential Work of Fracture (EWF) method, Eng. Fract. Mech. 204 (2018). https://doi.org/10.1016/j.engfracmech.2018.09.026.

[82] C.M. Chaléat, P.J. Halley, R.W. Truss, Properties of a plasticised starch blend. Part 1: Influence of moisture content on fracture properties, Carbohydr. Polym. 71 (2008). https://doi.org/10.1016/j.carbpol.2007.06.029.

[83] I. Yakimets, N. Wellner, A.C. Smith, R.H. Wilson, I. Farhat, J. Mitchell, Effect of water content on the fracture behaviour of hydroxypropyl cellulose films studied by the essential work of fracture method, Mech. Mater. 39 (2007). https://doi.org/10.1016/j.mechmat.2006.08.003.

[84] K.P. Plucknett, V. Normand, Plane stress essential work of fracture of "pseudo-ductile" gelatin/maltodextrin biopolymer gel composites, Polymer (Guildf). 41 (2000) 6833–6841. https://doi.org/10.1016/S0032-3861(00)00041-0.

[85] E.C.Y. Ching, W.K.Y. Poon, R.K.Y. Li, Y.-W. Mai, Effect of strain rate on the fracture toughness of some ductile polymers using the essential work of fracture (EWF) approach, Polym. Eng. Sci. 40 (2000) 2558–2568. https://doi.org/10.1002/pen.11386.

[86] T. Bárány, F. Ronkay, J. Karger-Kocsis, T. Czigány, In-plane and out-of-plane fracture toughness of physically aged polyesters as assessed by the essential work of fracture (EWF) method, Int. J. Fract. 135 (2005). https://doi.org/10.1007/s10704-005-3947-2.

[87] S. Hashemi, Fracture toughness evaluation of ductile polymeric films, J. Mater. Sci. 32 (1997). https://doi.org/10.1023/A:1018582707419.

[88] F.A. Pfaff, Growing more ductile epoxies: An essential work of fracture study, J. Coatings Technol. Res. 4 (2007). https://doi.org/10.1007/s11998-007-9013-4.

[89] M.L. Maspoch, O.O. Santana, J. Grando, D. Ferrer, A.B. Martinez, The essential work of fracture of a thermoplastic elastomer, Polym. Bull. 39 (1997). https://doi.org/10.1007/s002890050145.

[90] J. Karger-Kocsis, Toward understanding the morphology-related crack initiation and propagation behavior in polypropylene systems as assessed by the essential work of fracture approach, J. Macromol. Sci. - Phys. 38 (B) (1999). https://doi.org/10.1080/00222349908248127.

[91] M. Sakai, T. Miyajima, M. Inagaki, Fracture toughness and fiber bridging of carbon fiber reinforced carbon composites, Compos. Sci. Technol. 40 (1991).

https://doi.org/10.1016/0266-3538(91)90083-2.